NANO LETTERS

Letter

pubs.acs.org/NanoLett

Chiral Electromagnetic Fields Generated by Arrays of Nanoslits

E. Hendry,*[,†] R. V. Mikhaylovskiy,[†] L. D. Barron,[‡] M. Kadodwala,[‡] and T. J. Davis[§]

[†]School of Physics, University of Exeter, Stocker Road, Exeter EX4 4QL, U.K.

[‡]School of Chemistry, Joseph Black Building, University of Glasgow, Glasgow G12 8QQ, U.K.

[§]CSIRO Materials Science and Engineering, Private Bag 33, Clayton, Victoria, 3168, Australia

Supporting Information

ABSTRACT: Using a modal matching theory, we demonstrate the generation of short-range, chiral electromagnetic fields via the excitation of arrays of staggered nanoslits that are chiral in two dimensions. The electromagnetic near fields, which exhibit a chiral density greater than that of circularly polarized light, can enhance the chiroptical interactions in the vicinity of the nanoslits. We discuss the features of nanostructure symmetry required to obtain the chiral fields and explicitly show how these structures can give rise to detection and characterization of materials with chiral symmetry.

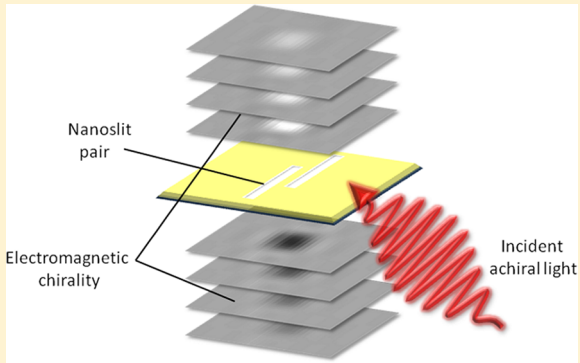

KEYWORDS: *Chirality, light scattering, nanophotonics, nano-optics, sensing*

Circular dichroic measurements are powerful probes of biomacromolecular structure[1] due to the intrinsic twist, or chiral symmetry, of circularly polarized radiation. However, the sensitivities of spectroscopic techniques which utilize circular dichroism are limited: for small chiral molecules, for example, the absorption cross sections for left- and right-circularly polarized light differ by less than one part per thousand.[2,3] This intrinsic weakness of chirally sensitive, or chiroptical, interactions arises from a mismatch between the chiral length scale of light (set by the wavelength of light), with the chiral length scale of molecule, which is typically orders of magnitude smaller.

Recently, it has been demonstrated that this natural ceiling to chiroptical sensitivity can be breached.[2,4,5] In ref 4, evanescent electromagnetic (EM) fields, created by scattering near chiral nanostructures, were used to significantly enhance the sensitivity of a chiroptical measurement. Here we develop a physical understanding of how chiral electromagnetic fields can be induced around nanostructures. We illustrate the principles using an exemplar structure of nanoslit pairs which maximize the chiral density of electromagnetic fields in localized regions of space. Subsequently, we develop models for describing the interaction of locally chiral fields with chiral media. This approach lays the foundations for practical applications of locally chiral electromagnetic fields in areas such has biomolecular characterization and sensing.

The origin of all chiroptical interactions lies in the symmetry of the light−matter interaction: due to the chiral symmetry of circularly polarized light, materials with an intrinsic twisted structure scatter inequivalently for left- and right-handed polarizations.[6] A crucial point in our work is therefore how to define the chirality of electromagnetic fields in a quantifiable manner. We follow the formalism developed by Tang and Cohen,[5] which defines the chirality of a time-varying electromagnetic field by considering the excitation rate of a "probe" molecule defined by point electric and magnetic dipole moments. For small molecules, chiroptical effects derive primarily from electric dipole−magnetic dipole coupling.[6] Beginning from the definitions of point dipoles, and using the behavior of electromagnetic fields under parity transformation, it is relatively straightforward to obtain the differential excitation rate between left- and right-handed systems.[5] For isotropic media with no preferential orientation in space, the dissymmetry in excitation rate can be written as

$$\Delta R = 2\omega G' \,\mathrm{Im}(\tilde{\mathbf{E}}^{(0)*}\cdot\tilde{\mathbf{B}}^{(0)}) \quad (1)$$

where G' describes the chiral optical properties of a molecule in the absence of an applied static magnetic field and $\tilde{\mathbf{E}}^{(0)}$ and $\tilde{\mathbf{B}}^{(0)}$ denote complex electric and magnetic vectors, respectively. ΔR represents the differential absorption (energy absorbed per second) of a molecule in left- and right-handed fields or indeed the differential absorption of mirror-image molecules in the same field. This asymmetry in energy absorption is intrinsically tied with an asymmetry in refraction/scattering via Kramers−Kronig relations. For bulk materials, this gives rise to absorption coefficients and refractive indices which are determined by the helicity of light. Equation 1 is a product of

Received: April 10, 2012
Revised: May 15, 2012
Published: May 17, 2012

   dx.doi.org/10.1021/nl3012787 | *Nano Lett.* 2012, 12, 3640−3644

a molecular property (G') with the chiral properties of the electromagnetic fields, given by

$$C = 2\omega\ \mathrm{Im}(\tilde{\mathbf{E}}^{(0)*}\cdot\tilde{\mathbf{B}}^{(0)}) \quad (2)$$

referred to here as electromagnetic chirality, a pseudoscalar that represents the intrinsic chiral symmetry of a time varying electromagnetic field. For a circularly polarized wave with unit intensity (i.e., magnitude of electric field vector $\sim 1/\sqrt{2}$), one can easily calculate the electromagnetic chirality of left ($C_L = +2\omega/c$) and right ($C_R = -2\omega/c$) circularly polarized light. We use these values to normalize all calculations below.

As pointed out separately by Bliokh and Nori[7] and Andrews and Coles,[8] the helicity of light is responsible for chiroptical interactions, so that circularly polarized light is unquestionably the most chiral form of electromagnetic waves. Nevertheless, eq 2 is valid for any time varying electromagnetic field (note that the ω/c terms in C_L and C_R, though equivalent to vacuum wavenumber, arise from derivatives of the electromagnetic fields in time). Can one generate a time varying electromagnetic field with greater chiral intensity than circularly polarized light? Enhanced evanescent fields, generated in the vicinity of scattering chiral nanostructures,[9] hold the key. It has recently been shown that the accustomed link between helicity and spin angular momentum breaks down for evanescent fields.[10] We show below that, by designing suitable scattering structures which increase electromagnetic intensity in the near field while simultaneously inducing a chiral symmetry to the fields, one can mediate chiroptical interactions. We show explicitly that chiral electromagnetic eigenmodes occur only for scattering nanostructures, which are themselves two-dimensionally chiral.

From eq 2 one can establish the essential property of local fields which possess chiral symmetry: the complex fields, $\tilde{\mathbf{E}}^{(0)}$ and $\tilde{\mathbf{B}}^{(0)}$, must be parallel and phase shifted, giving rise to a nonzero imaginary component to their dot product. This corresponds to real electric fields which have components parallel to the time derivative of the magnetic field. However, the radiation scattered from a single nanostructure is predominantly electric dipole radiation, and the electric and magnetic fields associated with such radiation are orthogonal—this is true for the near- and far-field zones.[11] From this we conclude that the electromagnetic eigenmodes of single nanoscale, achiral particles can never be chiral. The solution lies in engineering chiral ensembles of simple nanostructures, such that the magnetic field from one nanostructure is parallel to the electric field from another nanostructure. This is a rather simple and effective approach to generate nanoscale electromagnetic chirality in local regions of space.

We begin by considering the fundamental resonances of nanorods and nanoslits (see Figure 1). The fundamental excitation of a nanorod is an electric dipole mode[12] with high electric field at the ends of the rod. On resonance, a current maximum (and corresponding maximum in magnetic field) is found at the center of the rod. A nanoslit (i.e., a long slit in a metal film) is the complementary structure[13] and gives rise to regions of high magnetic field toward the ends of the nanoslit and a maximal electric field in the center. Both structures are resonant when the wavelength of incident light is approximately twice the length of the slit/rod. While the general principles under discussion here apply to both nanorods and nanoslits, we will concentrate for simplicity on nanoslit arrays. Though nanoslits do not possess chiral symmetry by themselves, one can arrange them in two-dimensional chiral ensembles by staggering them. To obtain a strong overlap between the electric and magnetic field regions, they can be arranged in pairs as shown in Figure 1b. While there are several ways in which this pairing can occur, only the chiral arrangement on the right-hand side of Figure 1b generates chiral fields: for this arrangement, both nanoslits can be excited simultaneously, and because of the fixed ($\pi/2$) phase relationship between electric and magnetic fields of the slit eigenmodes, electromagnetic chirality is generated in the regions where electric and magnetic fields overlap.

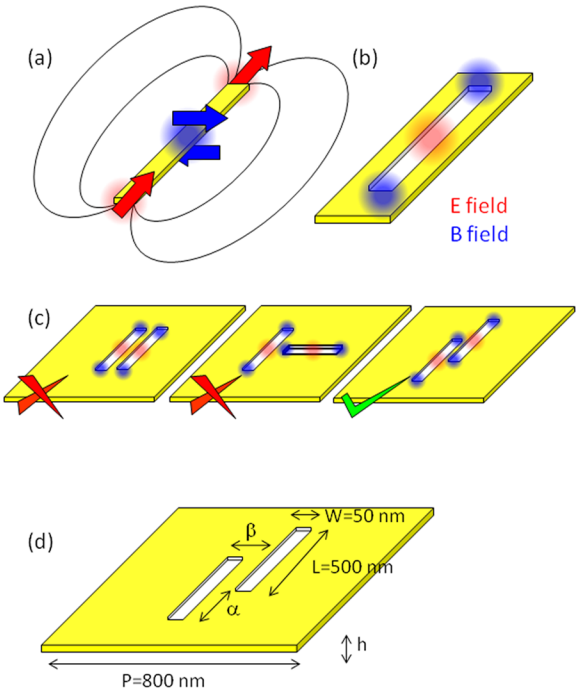

Figure 1. (a) Dipole resonance of a nonorod, highlighting regions of enhanced electric and magnetic fields. (b) Dipole resonance of a nanoslit. (c) Pairing arrangements of nanoslits. Only the arrangement on the right will exhibit chiral electromagnetic eigenmodes. (d) Dimensions of the chiral nanoslit arrays studied here.

In order to better understand the electromagnetic properties of our nanoslit pairs, we introduce a modal matching model based on that in refs 14−16. We describe in brief the method: the electromagnetic fields in the superstrate (incident) and substrate (transmission) regions, written as periodic Fourier−Floquet expansions, are matched to the fields of the waveguide modes inside the nanoslits. By exploiting continuity of electric and magnetic fields at the boundaries, we can obtain explicit analytical expressions for the electromagnetic fields in all regions of space. The full details of the model can be found in the Supporting Information. An important approximation lies with the description of the metal, treated here as perfectly conducting (i.e., effects due to field penetration into the metal, such as joule heating, are neglected). The nanoslit pairs are investigated as part of a periodic array of pitch 800 nm. Unless otherwise stated, we discuss the results for the dimensions shown in Figure 1c: slit length = 500 nm, slit width = 50 nm, height (h) = 50 nm, and lateral displacements α = 250 nm and β = 40 nm (see Figure 1d).

One of the defining properties of chiral structures is a different response to excitation by left- and right-handed circularly polarized light. The nanoslit arrays considered here are an example of a 2D chiral structure.[17] For finite h, a nonzero

dx.doi.org/10.1021/nl3012787 | Nano Lett. 2012, 12, 3640−3644

differential transmission of left- and right-handed light is observed, an effect arising from their intrinsically nonlocal response.[18] This is seen in Figure 2a, where we plot the

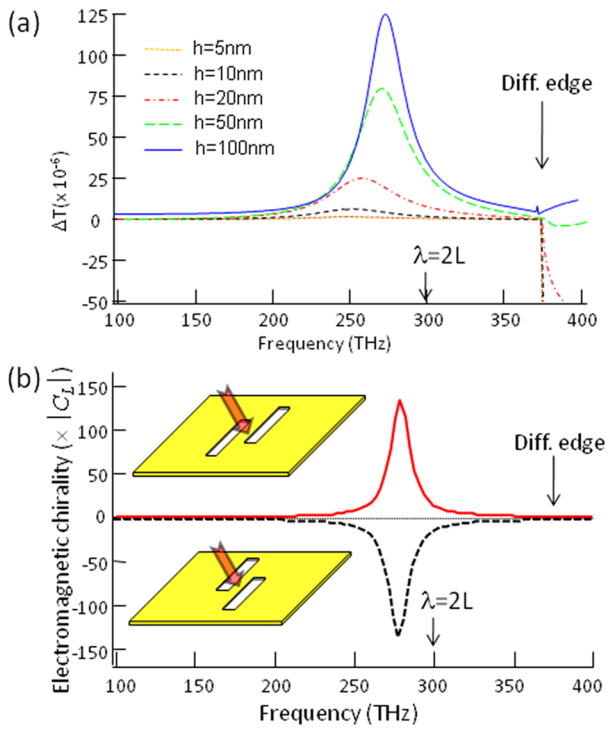

Figure 2. (a) Differential transmission, $\Delta T = T_L - T_R$, for arrays of different thickness h. (b) Local electromagnetic chirality determined in the center of the 2-dimensional unit cell, 1 nm above the transmission interface of the array (marked by arrow). The black (dashed) line shows the electromagnetic chirality for the mirror-imaged structure.

differential transmission spectrum of left- and right-handed incident light, $\Delta T = T_L - T_R$, for different h. The nanoslits exhibit a resonance in differential transmission at a wavelength that is approximately twice the length of the nanoslit. In addition to the resonance peak in differential transmission, a step change in the spectrum occurs on increasing frequency beyond the diffraction edge, marked by an arrow. This behavior occurs for frequencies where the structure is diffracting, due to the introduction of an additional radiative loss channel.[19]

Chiral arrays of nanoslits also generate local electromagnetic fields which are chiral. In Figure 2b, we plot the electromagnetic chirality generated at the fundamental resonance frequency of the nanoslits, calculated in the overlap region on the transmission side of the array (marked by the arrow at the center of the unit cell) for excitation by incident wave polarized perpendicular to the slit axis. The local electromagnetic chirality in this region is more than 2 orders of magnitude greater than that for circularly polarized light. The chiral selectivity of the local field, proportional to $\mathbf{C}/|\tilde{\mathbf{E}}^{(0)}|^2$,[5] is also spatially inhomogeneous and typically a few times that of circularly polarized light in the vicinity of the nanoslits. These chirality hotspots (i.e., with local electromagnetic fields which are simultaneously intense and chiral) do not arise from enhanced electromagnetic intensity alone but require phase shifted but parallel components of $\tilde{\mathbf{E}}^{(0)}$ and $\tilde{\mathbf{B}}^{(0)}$ fields in the same region of space. These locally chiral fields exhibit no intrinsic rotation of vector fields in space, a fundamental difference compared to circularly polarized light. The requirement of a fixed phase relationship between $\tilde{\mathbf{E}}^{(0)}$ and $\tilde{\mathbf{B}}^{(0)}$ fields gives rise to another interesting effect: the chirality of local evanescent field is determined by the symmetry of the nanostructures themselves. It is also important to stress that the handedness (and hence polarity) of the local electromagnetic chirality is *independent of the handedness of the incident light*. This behavior is in contrast to the planar cavities described in refs 2 and 5, where the polarity of the electromagnetic chirality is determined by that of the incident light.[7] The importance of nanostructure symmetry is therefore a defining feature of the resonant enhancements discussed here: the local electromagnetic chirality can be altered and tuned by modifying the structure itself—we return to this point below—and the mirror-imaged structure generates local fields with a reversed sense of chiral symmetry (see Figure 2b).

It is also clear that enhancement of electromagnetic chirality is a local effect, occurring only in regions very near the scattering structures. In Figure 3, it can be seen that the

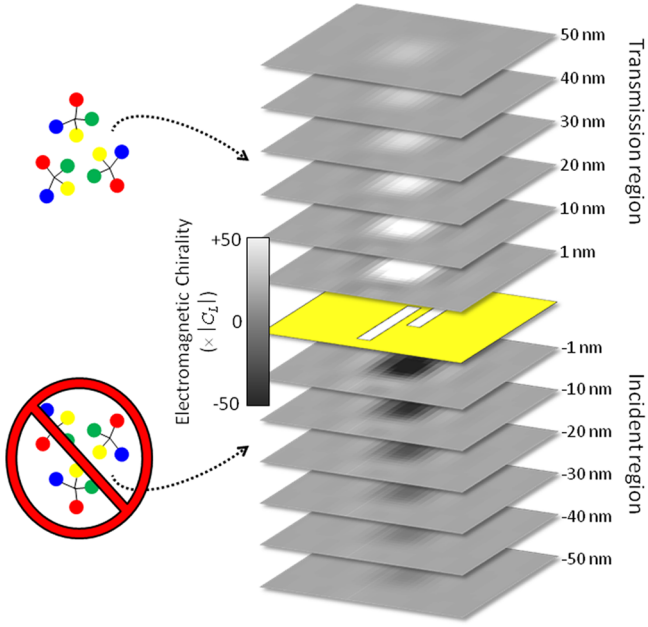

Figure 3. Spatially inhomogeneous electromagnetic chirality for excitation by incident wave polarized perpendicular to the slit axis. A chiral medium should be introduced in only one half-space (discussed here in the transmission region) to avoid cancelation due to the opposing polarity of electromagnetic chirality.

electromagnetic chirality decays exponentially with distance from the surface. Moreover, the electromagnetic chirality changes polarity on translation from superstrate to substrate sides of the array. An interesting observation is that, for thin structures ($h \rightarrow 0$), the integrated electromagnetic chirality over superstrate and substrate regions is equal to that of the incident light. This implies that, in the absence of absorption, electromagnetic chirality may be a conserved quantity, as suggested by Tang and Cohen.[5]

In local regions exhibiting high electromagnetic chirality one can probe chiroptical effects, as chiral materials in the vicinity of such twisted nanostructures will display amplified chiral asymmetry in their optical properties. For example, left-handed molecules will exhibit different excitation, emission, and scattering cross sections from their right-handed counterparts. Correspondingly, chiral molecules in the vicinity of left- and right-handed nanostructures are predicted to exhibit asymmetry

dx.doi.org/10.1021/nl3012787 | *Nano Lett.* 2012, 12, 3640−3644

in their optical behavior. In order to enhance chiroptical asymmetry in chiral materials, it is important to note that the chiral medium must be introduced in only one half-space (either substrate or superstrate) to avoid cancelation due to the opposing polarity of electromagnetic chirality in each region (see Figure 3). There are several means by which one could, at least in principle, observe such chiroptical interactions. In ref 4 an experiment to ascertain this asymmetry was demonstrated. In brief, chiral gold nanostructures were fabricated on quartz substrates, which were subsequently incorporated into a liquid cell for spectroscopic measurement. A circular dichroism spectrometer recorded the differential transmission spectrum, ΔT. Resonance frequency shifts were recorded due to molecular species adsorbed onto the metallic nanostructures with asymmetry for left- and right-handed nanostructures; i.e., when we reverse the chiral symmetry of the nanostructure with respect to that of the molecular species, one observes a relative shift in the resonance frequency. One can now understand the origin of this effect from Figure 2b: when the symmetry of a chiral nanostructure is changed to its mirror image, the polarity of the electromagnetic chirality is also reversed.

In order to elucidate the experimental findings in ref 4, we develop our model to describe the interaction of chiral local fields with chiral media. Since there are many types of chiral media in nature, we concentrate here on the simplest case: isotropic chiral materials. In such materials, a wave of given circular polarization propagates with the same wavenumber regardless of its direction of propagation. We therefore define in our model a material with a chiral refractive index component, Δn, so that the total, isotropic refractive index is different for left- and right-handed wave components, described by $n_{\pm} = n_0 \pm \Delta n$. Then, by deconvolving our Fourier–Floquet expansions in terms of left- and right-handed wave components, we can incorporate the effects of a chiral refractive index. It is important to note that this formulation includes the response of the nonabsorbing chiral medium to the evanescent, nonradiative field components. It is these evanescent fields that give rise to handedness through their different amplitudes for spin-polarized field components (see Supporting Information). Details of this procedure are supplied in the Supporting Information. By defining a chiral component to the refractive index in the transmission region of the nanostructure array, we distinguish resonance shifts which are qualitatively similar to those observed in experiment:[4] the black line in Figure 4a represents the dipole resonance of the nanoslit arrays in the presence of an achiral material with refractive index, $n_0 = 1.5$, while the blue (dotted) and red (dashed) lines represent the resonance with a chiral component of refractive index introduced on the transmission side of the array, defined by $\Delta n = +0.03$ and $\Delta n = -0.03$, respectively. The dotted and dashed lines therefore represent systems in which the chiral symmetry of the material in the transmission region is reversed with respect to the chiral nanostructure. The resonance shift also increases as the chiral refractive index component increases in magnitude. As expected, we observe similar effects when a chiral medium is introduced in the incident rather than transmission region, with frequency shifts reversed in sign.

One important aspect of nanostructure induced electromagnetic chirality is that local electromagnetic chirality can be tuned through the structure of the nanostructure array. In Figure 4b, we plot the frequency shifts (measured at half-maximum of the peak) as a function of the array parameter α (see Figure 1). The local electromagnetic chirality at the

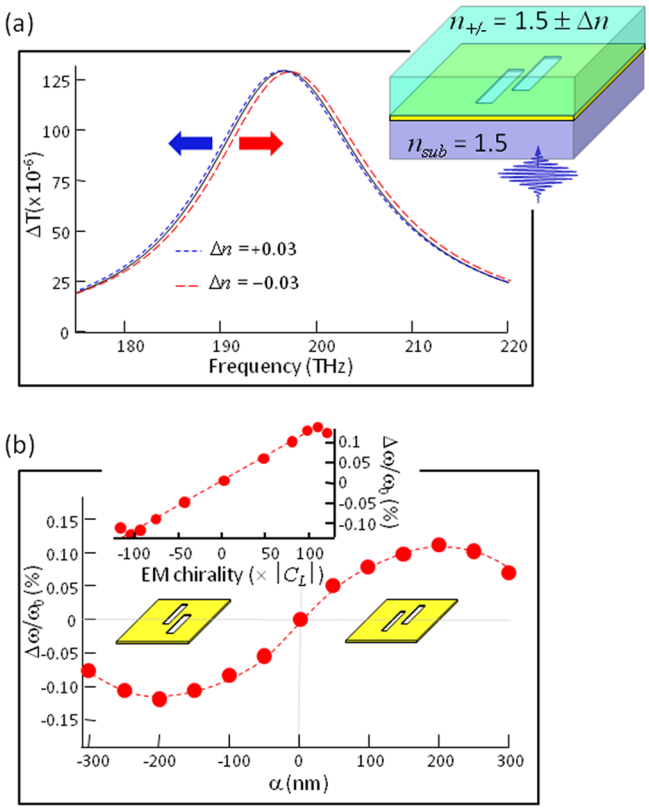

Figure 4. (a) Solid (black) line: differential transmission for a chiral array of nanoslits immersed in a medium with a refractive index of 1.5. Dotted (blue) and dashed (red) lines display differential transmission with a chiral medium in the transmission region, defined by defined by $\Delta n = +0.03$ and $\Delta n = -0.03$, respectively. (b) Resonance shifts as a function of array parameter α. Inset: correlation between resonance shift, normalized by the resonant frequency (ω_0), and electromagnetic chirality, determined at point marked in Figure 2b.

transmission interface of the array is strongly dependent on α, as the overlap integral of electric and magnetic field components is modified. Moreover, the sign and magnitudes of the resonance shifts observed in Figure 4a are correlated to the electromagnetic chirality generated by the nanostructures (see inset of Figure 4b). We see similar effects for higher order (quadrupolar) nanoslit modes (see Supporting Information).

An important point to note is that the spectral shifts in Figure 4, for refractive indices of typical chiral liquids,[20] are *significantly smaller than observed in experiment.*[4] This indicates that there may be other mechanisms of enhancement at work. This is most likely due to a combination of factors. First, adsorbed molecules may influence the electronic states of the metallic nanostructures.[21] Furthermore, molecular alignment at the substrate interface may play an important role, giving rise to aligned dipole–dipole interactions[22] or contributions to chiroptical phenomena through electric dipole–electric quadrupole coupling.[6] Finally, for large biomolecules which are of the same order as the spatial decay length of the inhomogeneous local electromagnetic fields, nonlocal effects may be important. We stress that eq 2 is only strictly correct for infinitely small chiral molecules, as the derivation begins with the assumption of point dipoles. For finite-sized molecules, the nature of the dipole–dipole interactions can be more complex and intrinsically nonlocal in nature. Under such circumstances, one can expect resonant scattering conditions due to the large

dx.doi.org/10.1021/nl3012787 | *Nano Lett.* 2012, 12, 3640–3644

wavevector components present in strongly inhomogeneous near fields.

In conclusion, we have developed a physical understanding of how nanostructures can generate chiral evanescent fields. Consequently, we have been able to determine the symmetry properties of a nanostructure required to optimize the chirality of the local electromagnetic fields. We then explicitly show how these structures can give rise to amplified response to media with chiral symmetry and developed a qualitative understanding of the phenomenon reported in ref 4. Our approach therefore lays the foundations for the practical applications in the detection of chiroptical materials such as biomolecular characterization and sensing.

■ ASSOCIATED CONTENT

Supporting Information

Formulation of our modal matching model, additional calculations of the quadrupole cavity resonance. This material is available free of charge via the Internet at http://pubs.acs.org.

■ AUTHOR INFORMATION

Corresponding Author

*E-mail: e.hendry@ex.ac.uk.

Notes

The authors declare no competing financial interest.

■ ACKNOWLEDGMENTS

This work was supported through funding from the EPSRC. The authors thank Ian Hooper for discussion on data analysis, and Harald Giessen, Konstantin Bliokh and Mike Wiltshire for useful discussions.

■ REFERENCES

(1) Chen, Y. H.; Yang, J. T.; Martinez, H. M. *Biochemistry* **1972**, *11*, 4120−4131.
(2) Tang, Y. Q.; Cohen, A. E. *Science* **2011**, *6027*, 333−336.
(3) Berova, N.; Nakanishi, K.; Woody, R. *Circular Dichroism: Principles and Applications*; Wiley: New York, 2000.
(4) Hendry, E.; Carpy, T.; Johnston, J.; Popland, M.; Mikhaylovskiy, R. V.; Lapthorn, A. J.; Kelly, S. M.; Barron, L. D.; Gadegaard, N.; Kadodwala, M. *Nat. Nanotechnol.* **2010**, *5*, 783.
(5) Tang, Y. Q.; Cohen, A. E. *Phys. Rev. Lett.* **2010**, *104*, 163901.
(6) Barron, L. D. *Molecular Light Scattering and Optical Activity*, 2nd ed.; Cambridge University Press: Cambridge, 2004.
(7) Bliokh, K. Y.; Nori, F. *Phys. Rev. A* **2011**, *83*, 021803(R).
(8) Coles, M. M.; Andrews, D. L. arXiv:1203.1755v1, 2012.
(9) Kitaev, V. *J. Mater. Chem.* **2008**, *18*, 4745−4749.
(10) Bliokh, K. Y.;Nori, F. 2012, arXiv:1201.2746v2.
(11) Jackson, J. D. *Classical Electrodynamics*, 2nd ed.; Wiley: New York, 1975.
(12) Jain, P. K.; Eustis, S.; El-Sayed, M. A. *J. Phys. Chem. B* **2006**, *110*, 18243−18253.
(13) Zentgraf, T.; Meyrath, T. P.; Seidel, A.; Kaiser, S.; Giessen, H.; Rockstuhl, C.; Lederer, F. *Phys. Rev. B* **2007**, *76*, 033407.
(14) McPhedran, R. C. *Electromagnetic Theory of Gratings*; Springer-Verlag: Berlin, 1980.
(15) Hendry, E.; Hibbins, A. P.; Sambles, J. R. *Phys. Rev. B* **2008**, *78*, 235426.
(16) Stone, E. K.; Hendry, E. *Phys. Rev. B* **2011**, *84*, 035418.
(17) Papakostas, A.; Potts, A.; Bagnall, D. M.; Prosvirnin, S. L.; Coles, H. J.; Zheludev, N. I. *Phys. Rev. Lett.* **2003**, *90*, 107404.
(18) Reichelt, M.; Koch, S. W.; Krasavin, A. V.; Moloney, J. V.; Schwanecke, A. S.; Stroucken, T.; Wright, E. M.; Zheludev, N. I. *Appl. Phys. B: Lasers Opt.* **2006**, *84*, 97−101.
(19) Prosvirnin, S. L.; Zheludev, N. I. *Phys. Rev. E* **2005**, *72*, 037603.
(20) Ghosh, A.; Fischer, P. *Phys. Rev. Lett.* **2006**, *97*, 173002.
(21) Ha, J. M.; Solovyov, A.; Katz, A. *Langmuir* **2009**, *25*, 153−158.
(22) Gérard, V. A.; Gun'ko, Y. K.; Defrancq, E.; Govorov, A. O. *Chem. Commun.* **2011**, *47*, 7383−7385.